

Aeration performances of a gabion stepped weir with and without capping

Davide Wuthrich · Hubert Chanson

Received: 25 February 2014 / Accepted: 25 July 2014 / Published online: 9 August 2014
© Springer Science+Business Media Dordrecht 2014

Abstract The stepped spillway design has been used for more than 3,300 years. A simple structure is the gabion stepped weir. A laboratory study was performed herein in a large size facility. Three gabion stepped weirs were tested with and without capping, as well as a flat impervious stepped configuration. For each configuration, detailed air–water flow measurements were conducted systematically for a range of discharges. The observations highlighted the seepage flow through the gabions and the interactions between seepage and overflow. The air–water flow properties showed that the air concentration, bubble count rate and specific interface data presented lower quantitative values in the gabion stepped weir, compared to those on the impervious stepped chute, while higher velocities were measured at the downstream end of the gabion stepped chute. The re-oxygenation rate was deduced from the integration of the mass transfer equation using air–water interfacial area and velocity measurements. The aeration performances of the gabion stepped weir were lesser than on the flat impervious stepped chute, but for the lowest discharge. For the two configurations with step capping, the resulting flow properties were close to those on the impervious stepped configuration.

Keywords Gabion stepped weirs · Aeration · Physical modelling · Air–water interfacial flow properties · Seepage flow · Impervious step capping · Stepped spillways · Re-oxygenation

1 Introduction

For a spillway system, the safe dissipation of the turbulent kinetic energy is uppermost important [26]. Among the energy dissipation systems, the stepped chute design is recognised

Electronic supplementary material The online version of this article (doi:[10.1007/s10652-014-9377-9](https://doi.org/10.1007/s10652-014-9377-9)) contains supplementary material, which is available to authorized users.

D. Wuthrich · H. Chanson (✉)
School of Civil Engineering, The University of Queensland, Brisbane, QLD 4072, Australia
e-mail: h.chanson@uq.edu.au
URL: <http://www.uq.edu.au/~e2hchans/>



Fig. 1 Aeration above a gabion stepped chute at Duralie Coal project (Australia) on 23 March 2005 (Courtesy of Tony MARSZALEK)

for its energy dissipation and flow aeration performances [5]. The stepped cascade design has been used for more than 3,300 years with the oldest stepped weir still standing in Greece [23]. Aeration on stepped spillways is a key feature linked to the strong flow turbulence, free-surface turbulent interactions and air entrainment [25,32] (Fig. 1). For the treatment of drinking water, cascade aeration can be used to reduce the chlorine content, offensive taste and odours [11]. Re-oxygenation cascades were also built downstream of dam spillways, and along rivers and canals [16, 18, 19]. The physical process of mass transfer is described by the Fick's law stating that the mass transfer rate across an interface varies proportionally to a diffusion coefficient times the gradient of gas concentration:

$$\frac{\partial M_{\text{gas}}}{\partial t} = -D_{\text{gas}} \times A \times \left(\frac{\partial C_{\text{gas}}}{\partial x} \right) \quad (1)$$

where M_{gas} is the mass of dissolved gas, t is the time, D_{gas} is the diffusion coefficient of the gas in the liquid, A is the gas-liquid interfacial area, C_{gas} is the concentration of the dissolved gas and x is the direction in which the diffusion occurs. For volatile gases, the equation for mass transfer across an air–water interface can be rearranged as

$$\frac{\partial C_{\text{gas}}}{\partial t} = K_L \times a \times (C_{\text{SAT}} - C_{\text{gas}}) \quad (2)$$

where K_L is the mass transfer coefficient or liquid film coefficient, a is the specific interface area defined as the interface area per unit volume, and C_{SAT} is the amount of gas dissolved in water at equilibrium [20]. The rate of mass transfer is directly proportional to the specific air–water interface area of the flow and therefore enhanced in highly aerated, turbulent flows [32].

For low- to medium-head hydraulic structures, the gabions may be a suitable construction material and the advantages of this type of construction include its stability, low cost, flexibility and porosity [1,5]. It may even be considered as a noise abatement option [2]. Following the early laboratory work of [30] on small size models, [27] investigated the flow

regimes and energy dissipation of gabion stepped weirs with 0.2 m step height. [22] argued the impact of seepage-free-surface flow interactions on gabion weir performances. To date no study recorded the two-phase air–water properties on gabion weirs and the design of re-aeration gabion stepped weirs remains based upon older empirical guidelines.

Herein the air–water turbulent flow properties above a gabion stepped weir were investigated systematically. Three gabion designs were tested, with and without capping, and their performances were compared systematically with a smooth impervious stepped weir. The measurements were conducted in a large facility with a channel slope angle of 26° (1V:2H). The focus herein was a detailed investigation of the air–water interfacial flow properties of gabion stepped weirs. It is the aim of this work to characterise the aeration potential in terms of dissolved oxygen of gabion stepped chutes. The contribution is complemented by five digital movies as electronic supplementary materials (Digital Appendix).

2 Physical modelling and experimental facilities

2.1 Presentation

Physical hydraulic models are commonly used during the design stages to optimise a hydraulic structure. In the model, the flow conditions must be similar to those in the prototype, but scale effects might take place in small-size models. A basic issue is the extrapolation of the laboratory data to full-scale structures and the selection of the dynamic similarity. In a dimensional analysis, the relevant parameters include the fluid properties and physical constants, the channel geometry and inflow conditions, the air–water flow properties including the entrained air bubble characteristics and interfacial area characteristics. For a gabion stepped weir in a rectangular channel, a simplified dimensional analysis leads to a number of relationships between the air–water (over)flow properties, fluid properties, boundary conditions and channel geometries:

$$\begin{aligned}
 & C, \frac{V}{V_c}, \frac{u'}{V_c}, \frac{F \times d_c}{V_c}, a \times d_c, \dots \\
 & = F_1 \left(\frac{x}{d_c}, \frac{y}{d_c}, \frac{z}{d_c}, \frac{d_c}{h}, \rho_w \times \frac{V \times D_H}{\mu_w}, \frac{g \times \mu_w^4}{\rho_w} \times \sigma^3, \frac{W}{d_c}, \theta, \frac{k'_s}{d_c}, Po, \dots \right) \quad (3)
 \end{aligned}$$

where C is the void fraction, V is the interfacial velocity, u' is a characteristic velocity fluctuation, F is the bubble count rate, a is the air–water specific interface area defined as the air–water interfacial area per unit volume, d_c and V_c are the critical flow depth and velocity respectively, x, y, z are respectively the longitudinal, normal and transverse coordinates, D_H is the hydraulic diameter, W is the channel width, h and l are the step height and length respectively, g is the gravity acceleration, θ is the chute slope, μ_w is the dynamic viscosity of water, ρ_w is the water density, σ is the surface tension between air and water, k'_s is the equivalent sand roughness height of the step boundary surface, Po is the gabion porosity. Equation (3) expresses the dimensionless air–water overflow properties at a location (x,y,z) as functions of the relevant dimensionless parameters, including Froude, Reynolds and Morton numbers. Indeed the dimensionless discharge d_c/h is proportional to a Froude number defined in terms of the step height: $d_c/h = (q/\sqrt{g \times h^3})^{2/3}$ where q is the water discharge per unit width. Note that the gabion grain size and mesh characteristics are implicitly accounted for by the equivalent sand roughness height k'_s and porosity Po .

Table 1 Air–water flow measurements on the gabion and flat impervious stepped weirs (Present study, $\theta = 26.6^\circ$, $h = 0.10$ m)

Configuration (1)	Q (m ³ /s) (2)	d _c /h (3)	Re (4)	Instrumentation (5)
Gabion stepped weir (h = 0.10 m, $\theta = 26.6^\circ$)	0.018	0.5	1.40×10^5	Dual-tip phase detection probe ($\varnothing = 0.25$ mm)
	0.037	0.8	2.83×10^5	
	0.059	1.1	4.57×10^5	
	0.076	1.3	5.87×10^5	
	0.095	1.5	7.28×10^5	
	0.114	1.7	8.78×10^5	
Capped gabion stepped weir (h = 0.10 m, $\theta = 26.6^\circ$)	0.018	0.5	1.40×10^5	Dual-tip phase detection probe ($\varnothing = 0.25$ mm)
	0.037	0.8	2.83×10^5	
	0.059	1.1	4.57×10^5	
	0.076	1.3	5.87×10^5	
	0.095	1.5	7.28×10^5	
	0.114	1.7	8.78×10^5	
Fully-capped gabion stepped weir (h = 0.10 m, $\theta = 26.6^\circ$)	0.018	0.5	1.40×10^5	Dual-tip phase detection probe ($\varnothing = 0.25$ mm)
	0.037	0.8	2.83×10^5	
	0.059	1.1	4.57×10^5	
	0.076	1.3	5.87×10^5	
	0.095	1.5	7.28×10^5	
	0.114	1.7	8.78×10^5	
Flat impervious stepped weir (h = 0.10 m, $\theta = 26.6^\circ$)	0.018	0.5	1.40×10^5	Dual-tip phase detection probe ($\varnothing = 0.25$ mm)
	0.037	0.8	2.83×10^5	
	0.059	1.1	4.57×10^5	
	0.076	1.3	5.87×10^5	
	0.095	1.5	7.28×10^5	
	0.114	1.7	8.78×10^5	

Q water discharge measured at the crest, Re Reynolds number defined in terms of the hydraulic diameter

In the present study, the Morton number was an invariant because the same fluids were used in model and prototype [7,28,34]. Similarly the chute slope ($\tan \theta = h/l$) and the channel width W were kept constant and all the measurements were conducted on the channel centreline. Thus Eq. (3) may be simplified into:

$$C, \frac{V}{V_c}, \frac{u'}{V_c}, \frac{F \times d_c}{V_c}, a \times d_c, \dots = F_2 \left(\frac{x}{d_c}, \frac{y}{d_c}, \frac{d_c}{h}, \rho_w \times \frac{V \times D_H}{\mu_w}, \frac{k'_s}{d_c}, Po, \dots \right) \quad (4)$$

A Froude similitude was herein developed and the experiments were conducted in a large size facility which operated at large Reynolds numbers (Table 1) with relatively large-size gabion material. These conditions may correspond to a 1:3 to 1:5 scale study of the gabion stepped weir shown in Fig. 1, thus ensuring that the extrapolation of the laboratory data to prototype conditions is unlikely to be adversely affected by scale effects, although it is acknowledged that the bubble sizes might be overestimated and the specific interface area underestimated.



Fig. 2 Gabion stepped weir laboratory model with skimming flow conditions

2.2 Experimental facility and instrumentation

The air–water flow measurements were conducted in a large stepped weir model. The weir consisted of a broad-crested weir followed by ten steps with 0.1 m height and 0.2 m length. The crest and chute were 0.52 m wide. A pump controlled with an adjustable frequency AC motor drive delivered the flow rate, allowing a very accurate discharge control. The water discharge was deduced from the upstream head above crest, measured with a pointer gauge, using the discharge calibration of [14].

Four stepped configurations were tested: a smooth impervious stepped chute and three gabion stepped chutes (Table 1). The flat stepped configuration consisted of ten smooth impervious steps made of marine ply. Each step was 0.10 m high and 0.20 m long (1V:2H). For the gabion configurations, ten identical gabions were installed above the smooth impervious steps (Fig. 2). Each gabion was 0.3 m long, 0.1 high and 0.52 m wide, made of fine $12.7 \times 12.7 \text{ mm}^2$ galvanised metallic mesh and filled with natural river pebbles. The pebbles (Cowra pearl) were sieved with 14 mm squares. The density of the dry material was 1.6 tonnes/m³ corresponding to a porosity $P_o \approx 0.35 - 0.4$. Some detailed hydraulic conductivity tests were conducted and the hydraulic conductivity of the gabions was estimated as $K \approx 10^{-1} \text{ m/s}$ [35]. The capped gabion stepped configuration was constructed by installing 6 mm thick plexiglass plates on the horizontal faces of steps 2–10. That is, the first gabion box at the downstream end of the broad crest was not capped, and this allowed water to seep directly into the first gabion. Each plexiglass plate was 0.195 m long and 0.51 m wide. All the step edges were identically shaped, with the plate sharp edge ending 6–7 mm before the gabion edge. The fully-capped gabion stepped configuration was identical to the capped gabion weir, but for the addition of a plexiglass plate covering both the crest of the weir and first gabion. Further details and photographs were reported in [35]. For all configurations, the stepped weir ended in a flat tailrace channel in which the flow was supercritical for all investigated flow conditions.

The air–water flow measurements were conducted with a dual-tip phase detection intrusive probe. Each tip had an inner tip diameter $\varnothing = 0.25 \text{ mm}$ and the longitudinal separation of probe tips was $\Delta x = 6.2 \text{ mm}$. The conductivity probe was mounted on a sturdy trolley and

the elevation in the direction perpendicular to the pseudo bottom formed by the step edges was controlled by a fine adjustment screw-drive mechanism equipped with a MitutoyoTM digital ruler (accuracy < 0.1 mm). The probe was excited by an electronic air bubble detector with a response frequency greater than 100 kHz. The probe signal output was sampled at 20 kHz per sensor for 45 s.

2.3 Experimental flow conditions

The experimental study was conducted systematically on all four stepped weir configurations. Flow visualisations were carried out for a wide range of discharges from 0.005 up to 0.115 m³/s. The air–water flow properties measured for a range of dimensionless discharges between $0.5 \leq d_c/h \leq 1.7$ corresponding to Reynolds numbers between 1.40×10^5 and 8.78×10^5 and encompassing two flow regimes : transition and skimming flows (Table 1). Herein d_c is the critical flow depth, h is the vertical step height and the Reynolds number was calculated in terms of the hydraulic diameter. The experimental flow conditions are summarised in Table 1.

3 Basic flow patterns

3.1 Presentation

On the gabion stepped spillway, a porous seepage flow regime was observed for very small discharges ($d_c/h < 0.3$). In the porous flow regime, the water seeped through the gabion materials. On the first gabion box, some infiltration was observed. A short horizontal seepage face was observed on each step and there was no overflow past the step edges. For the smallest discharges, no vertical seepage was observed through the step vertical face. With increasing discharge, some small water jets came out of the gabions. The transition between porous and nappe flow regimes occurred once some overflow took place at the first gabion. The nappe flow ($0.3 < d_c/h < 0.6$) exhibited a succession of free falling nappes from one step edge to the next one. The cavity behind the nappe was filled with a superposition of seepage jets coming out of the upstream gabion (Fig. 3a). For example, the movie IMGP4633.avi illustrates the interactions between seepage and overflow for $d_c/h = 0.5$. In the lower cavity region, the recirculation motion exhibited a different pattern compared to that observed on flat impervious stepped spillways. A transition flow regime was observed for $0.6 < d_c/h < 0.9$. The hydrodynamic instabilities and splashes appeared less intense than on flat stepped spillways. The movie IMGP4537.avi shows the step cavity motion for $d_c/h = 0.85$, and some red wool strings helped to visualise the cavity flow patterns. For the largest discharges, a skimming flow was observed ($d_c/h > 0.90$). The flow pattern was generally similar to that observed on the flat stepped configuration (Fig. 4). However a different streamline pattern was seen next to the stagnation point on the horizontal step face (Fig. 5). Some bubbly flow and air bubble entrainment into the gabions were observed, mostly in the upper corner of each gabion box downstream of the inception point of free-surface aeration. Further differences were found in terms of cavity flow motion as a result of seepage flow effect. Detailed string studies were carried out to visualise the cavity flow (Fig. 5 & movie IMGP4566.avi). A vertical flow of air bubbles was observed close to the vertical step face. In the centre of the cavity a clear water core was seen in all cavities downstream of the inception point for all discharges (Fig. 4). The existence of a similar clear water core was previously reported by [17] for rough impervious steps. On the gabion stepped weir, some continuous interaction between the cavity and the gabion was noted.

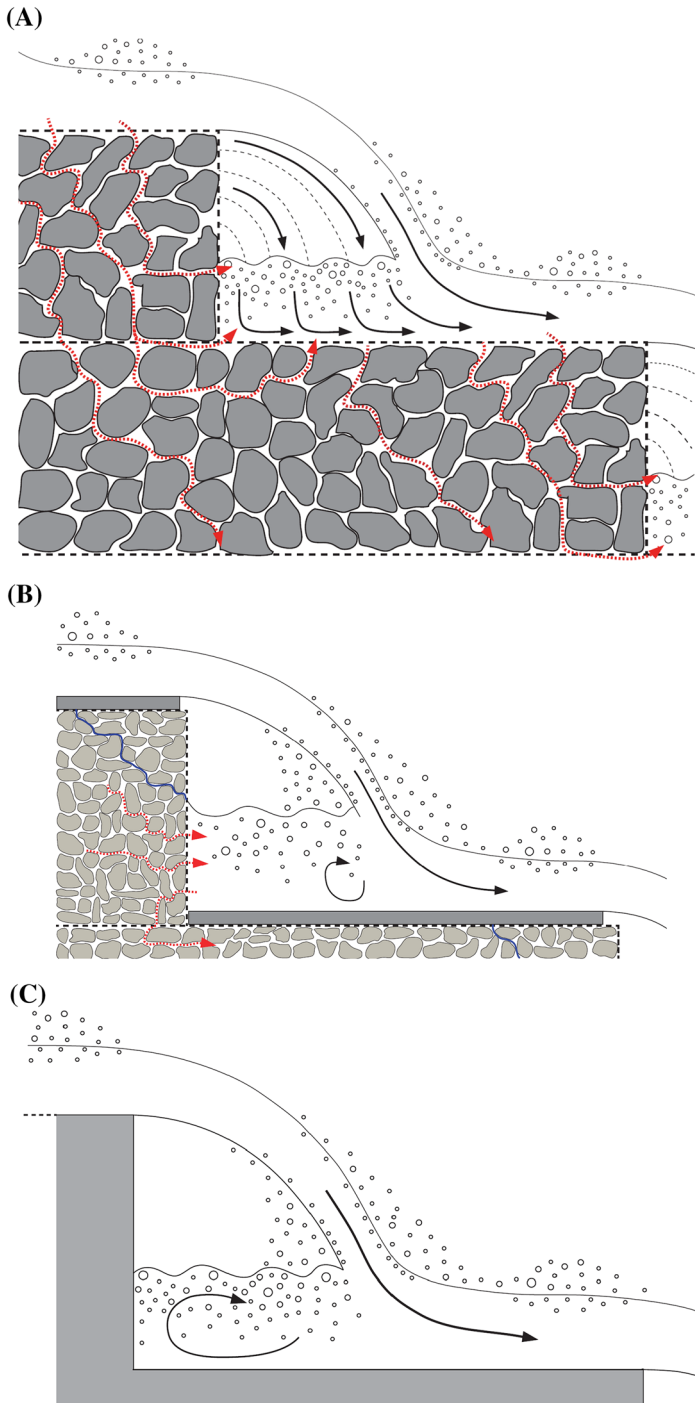


Fig. 3 Definition sketches of nappe flow on the gabion, capped gabion and flat impervious stepped weirs: *Red dotted arrows* show the bubbly seepage flow motion. **a** Nappe flow on gabion steps and bubbly motion in the gabions; **b** capped gabion steps; **c** flat impervious steps

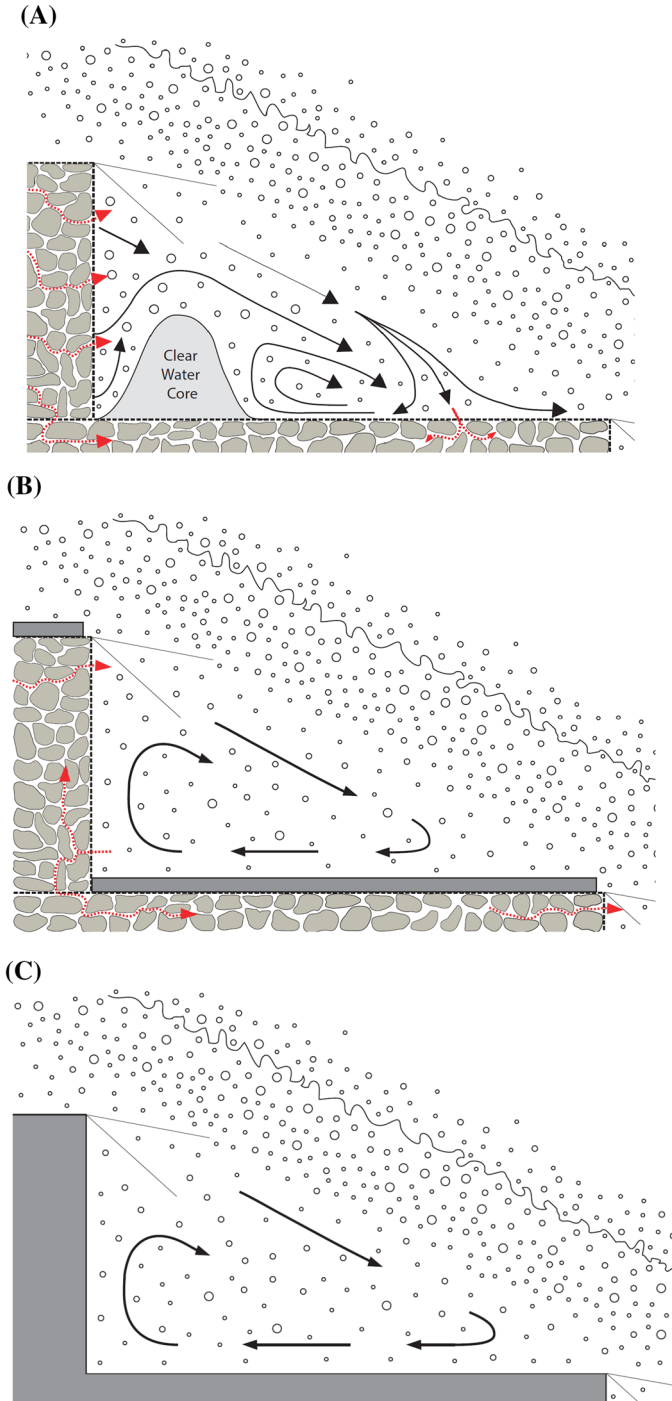


Fig. 4 Definition sketches of skimming flow on the gabion, capped gabion and flat impervious stepped weirs: *Red dotted arrows* show the bubbly seepage flow motion. **a** Gabion steps; **b** capped gabion steps; **c** flat impervious steps



Fig. 5 Cavity flow pattern in a skimming flow on gabion stepped weir - Flow conditions: step cavity 7–8, $Q = 0.068\text{m}^3/\text{s}$, $d_c/h = 1.20$, $Re = 5.2 \times 10^5$ - Note the clear water core in the step cavity

On the capped gabion stepped chute, a porous regime was observed for $d_c/h < 0.20$. For larger discharges, a nappe flow regime was seen for $0.20 < d_c/h < 0.60$, a transition flow for $0.60 < d_c/h < 0.90$, and the skimming flow for $d_c/h > 0.90$. In these flow regimes, the flow patterns were similar to those observed on the flat impervious stepped chute. Some differences were noticed at cavity level as a consequence of the seepage flow through the gabions. This is sketched in Figs. 3b and 4b. The effect of the seepage flow was mostly noticeable for the small discharges, i.e., for the porous and nappe flow regime. The skimming flow did not appear to be much influenced by the seepage flow. The movies IMG5407.avi and IMG5001.avi illustrate the cavity flow motion and interactions between seepage and cavity flow for a nappe and skimming flow respectively. On the fully capped gabion stepped configurations, the flow patterns were generally close to those observed on the flat impervious stepped chute and capped gabion stepped weir, but for the first step cavity. The changes in flow regimes are summarised in Table 2 and compared with other configurations.

On the flat impervious stepped weir, a nappe flow regime was observed for the smallest discharges ($d_c/h < 0.5$) (Fig. 3c). The flow consisted of a succession of free falling nappes. Below each water jet, a recirculating pool of water was formed with a clearly-defined air cavity above. For a range of intermediate discharges ($0.5 < d_c/h < 0.9$), the flow was characterised by strong hydrodynamic instabilities associated with a well developed spray region and a large amount of splashes [9]. For the larger discharges ($d_c/h > 0.9$), the flow skimmed as a coherent stream above the pseudo-bottom formed by the step edges. Substantial air entrainment occurred downstream of the inception point of free surface aeration, and an energetic recirculation pattern was observed in the step cavities as discussed by [24,29] and [10] (Fig. 4c). The observations and conditions for the changes between flow regimes are listed in Table 2 and they were close to the relevant literature for this chute slope.

3.2 Air entrainment within the gabions

A key difference between the flat impervious and gabion stepped weirs was the seepage motion and entrainment of air bubbles inside the gabions. For all porous configurations,

Table 2 Changes in stepped chute flow regimes on gabion and rough stepped chutes

Ref.	θ (°)	h (m)	Configuration	d_c/h		
				PR-NA	NA-TRA	TRA-SK
Present study	26.6	0.10	Flat impervious	N/A	0.5	0.9
			Gabion	0.3	0.6	0.9
			Capped gabion	0.2	0.6	0.9
			Fully-capped gabion	N/A	0.5	0.9
Gonzalez et al. [17]	21.8	0.10	S - Smooth steps	N/A	0.64	0.97
			A - Rough steps	N/A	0.64	0.97
			B - Rough vertical step faces	N/A	0.64	0.97
			C = Rough horizontal step faces	N/A	0.64	0.97

NA nappe flow, PR porous flow regime, TRA transition flow, SK skimming flow

air bubbles were seen flowing through the gravel (see movies). The Electronic Appendix regroups a series of HD digital video movies of bubbly flow motion in the gabions. The largest amount of bubble motion inside the gabions was observed in the gabion stepped structure for a given overflow rate. Lesser air entrainment in gabions was seen in the capped and fully-capped stepped configurations for an identical flow rate. With a nappe (over)flow regime, a large amount of bubbles moved inside the top edge of the gabions (Fig. 3b & movie IMGP4633.avi). A majority of bubbles flowed through the gabions and into the downstream step cavity. Some collided with gravel particles and emerged into the cavity by buoyancy. A few bubbles flowed through the gravel into the downstream gabion box. With increasing discharges, the upstream gabion boxes became water saturated and no bubble was observed. For the larger discharges with transition and skimming (over)flows, an inception point of gabion aeration was clearly observed. The location basically coincided with the apparition of air bubbles in the step cavities. Downstream, bubbles were entrained into the gabions. In the skimming flow regime, a modification of the streamlines impacting onto the horizontal step face was observed. It resulted in some bubbly flow into the upper edge of the gabion as sketched in Fig. 4a (also Fig. 5 & movie IMGP4566.avi).

With both capped and fully-capped gabion stepped configurations, some bubble motion inside the gabions was also observed, although the impervious capping affected the seepage motion. Both configurations presented very similar patterns. For the nappe (over)flow regime, the upper edge of each gabion box was unsaturated and a free surface was clearly identified (Fig. 3b & movie IMGP5407.avi). Some bubbles were seen flowing in the saturated gabion material. The amount of entrained bubbles inside the gabions appeared to be reduced compared to the gabion stepped configuration. In the skimming flow regime, a majority of gabion bubbles came from the cavity-gabion interactions along the vertical step face since the horizontal step face was capped (Fig. 4b). The cavity recirculation motion tended to push air bubbles inside the gabion. The gabion bubbles either moved up or down to the downstream gabion box (Fig. 4b & movie IMGP5001.avi). The latter (downward) bubbly motion tended to flow horizontally beneath the capping and between the capping and metallic mesh wire. Differences between capped and fully-capped stepped configurations were mostly seen in the first gabion box and first step cavity.

4 Air–water flow properties

4.1 Basic properties

All the void fraction data showed a substantial flow aeration. Overall the nappe flows over gabion steps were slightly less aerated than the flow on the flat impervious stepped weir. However the air concentration at $y = 0$ (i.e. at the gabion edge) was non-zero because of the bubbly flow inside the gabions. In the skimming flows, the void fraction data exhibited a S-profile (Fig. 6a). In Fig. 6, y is the distance normal to the pseudo-bottom formed by the step edges, and d_c and V_c are the critical flow depth and velocity respectively. The flow aeration tended to be lesser on the gabion stepped chute than on the smooth impervious stepped chute for the same flow rate. The void fraction distributions were successfully compared with the advective diffusion equation (not shown) [8].

The bubble count rate distributions on all gabion and flat impervious stepped configurations showed a marked maximum corresponding to a local void fraction between 0.4 and 0.5 (Fig. 6b). For all discharges, the bubble count rate was consistently smaller on the gabion stepped weir compared to the flat impervious stepped chute. The relationship between void fraction and bubble count rate was tested for all flow conditions at all step edges. Although the data indicated a pseudo-parabolic relationship [4, 8, 31], a more advanced theoretical model was applied [31, 33]:

$$\frac{F}{F_{\max}} = \frac{1}{\alpha \times \beta} \times \frac{C \times (1 - C)}{C_{F_{\max}}^2} \quad (5)$$

where F_{\max} is the maximum bubble rate in a cross-section, and α and β are two correction factors which are functions of the local void fraction and flow conditions, and $C_{F_{\max}}$ is the void fraction for which $F = F_{\max}$. Further details on the theoretical model (Eq. (5)) are presented in Appendix I. Some typical results are shown in Fig. 7 where Eq. (5) is compared with experimental data and a simplified parabolic relationship. Equation (5) compared favourable with the data on all gabion and flat impervious stepped weir data.

The velocity distributions showed some self-similar profiles which compared well with a 1/10th power law for $y < Y_{90}$ where Y_{90} is the characteristic elevation where $C = 0.90$. In the nappe flow regime, the interfacial velocities were smaller on the gabion steps for the same flow rate. Some typical results in the skimming flow regime are presented in Fig. 6c, illustrating that the gabion stepped chute flow exhibited faster velocities than the smooth impervious stepped chute flow, for the same discharge at the same location downstream of the inception point of free-surface aeration. The capped and fully-capped gabion chute data showed intermediate results between the gabion and flat impervious chute data. The result was counter-intuitive, although a similar trend was previously observed on rough impervious steps by [17] and [3].

4.2 Longitudinal distributions of characteristic air–water flow parameters

Some typical longitudinal distributions of characteristic air–water properties are presented in Fig. 8. The data include the depth averaged void fraction C_{mean} , the characteristic air–water flow velocity V_{90} and the depth averaged specific interface area a_{mean} . C_{mean} and a_{mean} were estimated respectively as [6, 8]:

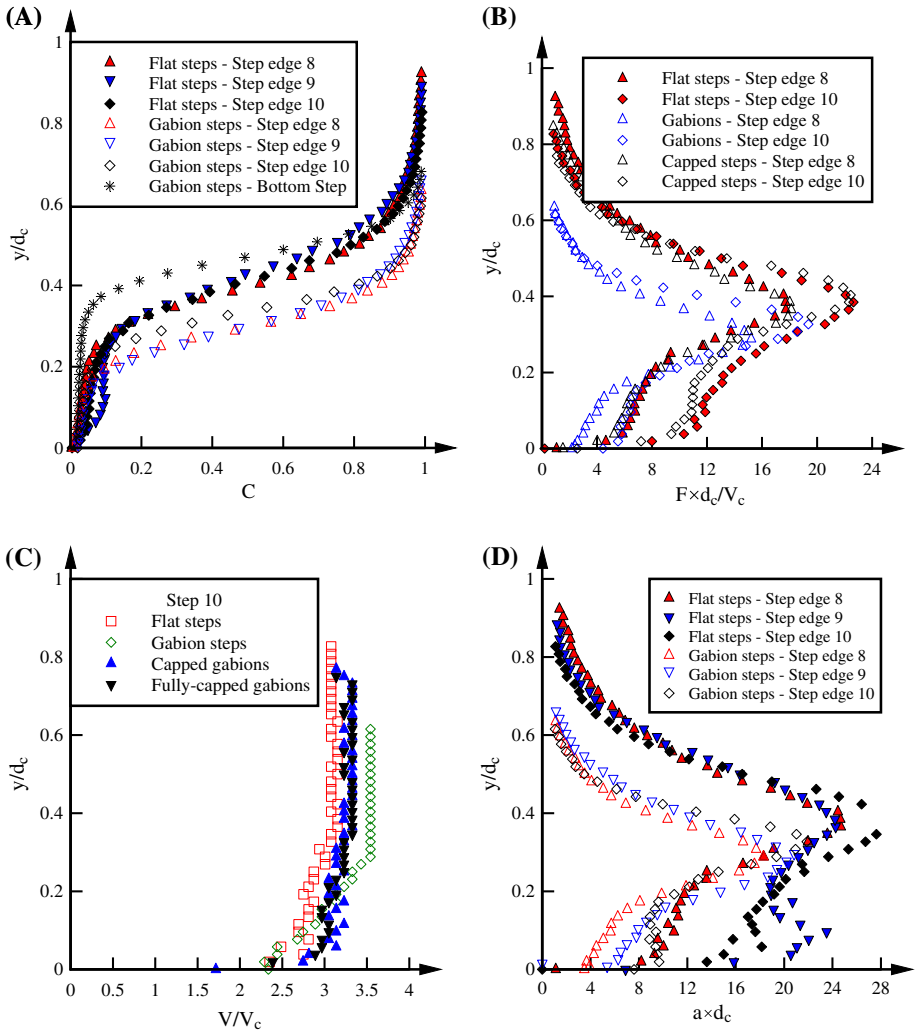


Fig. 6 Air water flow properties on gabion and flat impervious stepped weirs: flow conditions: Skimming flow regime, $d_c/h = 1.3$, $Q = 0.076\text{m}^3/\text{s}$, $Re = 5.9 \times 10^5$. **a**, Left Dimensionless distributions of void fraction: comparison between gabion (*empty symbols*) and flat impervious (*filled symbols*) stepped chute data; **b**, Right Dimensionless distributions of bubble count rate: comparison between gabion (*blue symbols*), capped gabion (*black symbols*) and flat impervious (*filled red symbols*) stepped chute data; **c**, Left) Dimensionless distribution of interfacial velocity at step edge 10: comparison between gabion, capped gabion, fully-capped gabion and flat impervious stepped chute data; **d**, Right) dimensionless distribution of specific interface area: Comparison between gabion (*empty symbols*) and flat impervious (*filled symbols*) stepped chute data

$$C_{\text{mean}} = \frac{1}{Y_{90}} \times \int_0^{Y_{90}} C \times dy \tag{6}$$

$$a_{\text{mean}} = \frac{1}{Y_{90}} \times \int_0^{Y_{90}} a \times dy \tag{7}$$

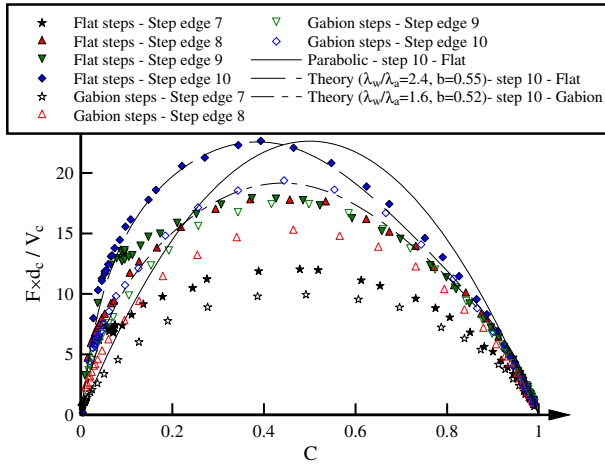


Fig. 7 Relationship between void fraction and bubble count rate on flat impervious and gabion stepped chute in skimming flow ($\theta = 26.6^\circ$)

where the specific interface area a in a turbulent air–water flow may be estimated as [6]:

$$a = \frac{4 \times F}{V} \tag{8}$$

with F the bubble count rate and V the interfacial velocity.

The experimental results are plotted in dimensionless form in terms of the step edge in Fig. 8. Note that an additional measurement (step 11) was included: it was set in the horizontal channel at the bottom of the stepped weir and located at 0.2 m downstream of step 10. The data highlighted a lesser aeration of the flow on the gabion stepped configuration (Fig. 8a). At step edge 10, C_{mean} was between 0 and 40 % larger on the flat impervious stepped weir than on the gabion weir. The characteristic velocity V_{90} data showed that, in the skimming flow regime, the velocities on gabion steps were larger than those on the flat smooth stepped configuration (Fig. 8b). The air–water flow properties on the capped and fully-capped gabion weirs tended to be in between the gabion and flat impervious stepped weir data.

4.3 Discussion

The porosity of gabion steps induced some seepage through the gabions, thus reducing the overflow discharge above the steps. The overflow discharge per unit width above the gabions was estimated by applying the equation of conservation of mass using the void fraction and velocity data. The results showed that the proportion of seepage flow was a function of the flow regime and flow rate. In skimming flows, it was about 15 % down to 5 % of the total flow rate with increasing discharge.

Cappings are introduced to enhance the abrasion resistance of gabions (Agostini et al. [1]; Peyras et al. [27]). Although they can be in bamboos and timber, modern cappings are commonly made out of steel sheets, concrete or reinforced concrete slabs. The present results showed that the introduction of impervious cappings above gabion steps led to an overflow pattern and air–water flow properties similar to those on a flat impervious stepped weir.

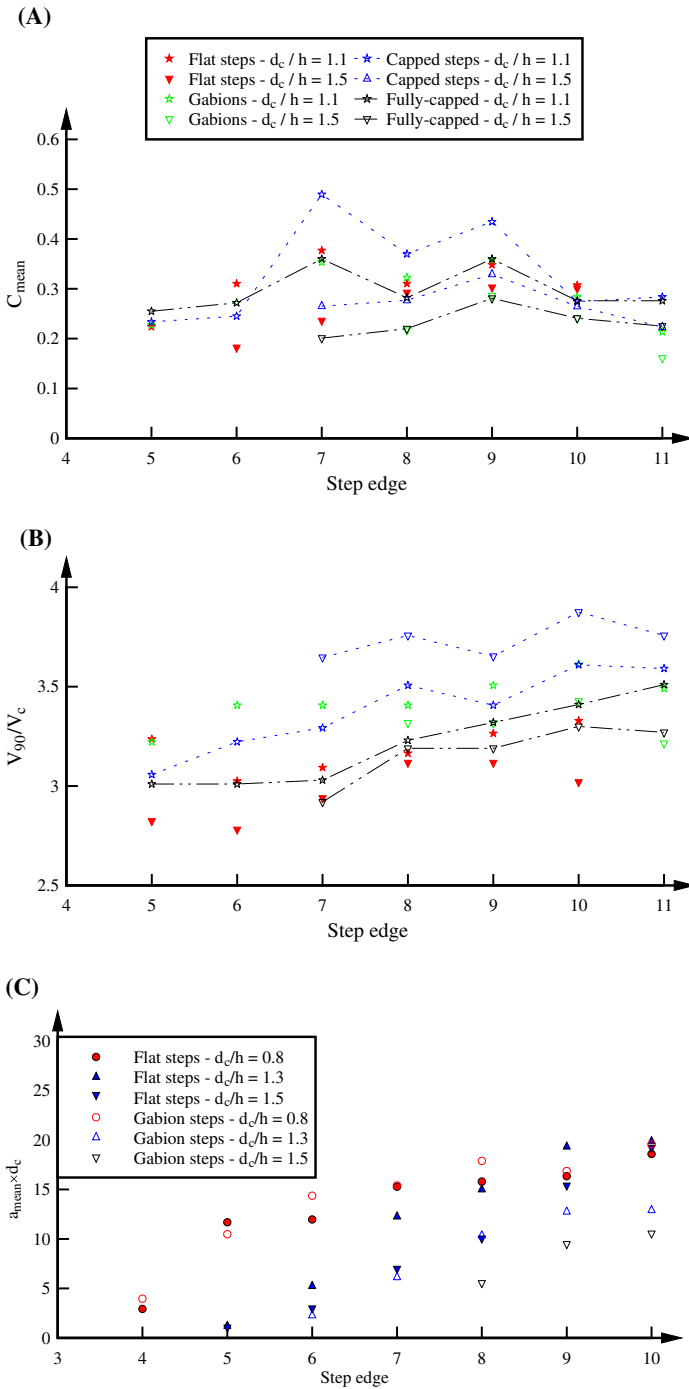


Fig. 8 Longitudinal distributions of characteristic air–water flow parameters on gabion, capped gabion and fully-capped gabion and flat impervious stepped weirs configurations ($\theta = 26.6^\circ$, $h = 0.10\text{m}$)—same legend for both graphs. **a** Depth-averaged void fraction C_{mean} ; **b** characteristic air–water velocity V_{90} —same legend as **a**; **c** depth-averaged specific interface area a_{mean}

5 Interfacial area and mass transfer rate

5.1 Specific interface area

The specific interface area represents the cumulative surface of air bubbles that is encountered per unit volume. In the present study, the specific interface area profiles were estimated for all four stepped weirs for a wide range of discharges ($0.05 < Q < 0.114\text{m}^3/\text{s}$) at all step edges downstream of the inception point of free-surface aeration. Some typical vertical distributions of specific interface area are shown in Fig. 7c. The data showed systematically a marked maximum corresponding to the location of maximum bubble count rate. Some typical longitudinal distributions of depth-averaged specific interface area are presented in Fig. 8c. The mean specific interface area increased monotonically with increasing distance downstream of the inception point of free-surface aeration. Overall the interface area levels were consistently smaller on the gabion stepped chute than on the flat impervious stepped weir (Figs. 7c, 8c).

5.2 Mass transfer rate

Considering a stepped chute, the rate mass transfer process may be derived from Fick’s law (Eq. (1)):

$$\frac{\partial C_{\text{gas}}}{\partial x} = \frac{K_L \times a_{\text{mean}}}{U_w} \times (C_{\text{SAT}} - C_{\text{gas}}) \tag{9}$$

where U_w is the flow velocity defined as:

$$U_w = \frac{q}{\int_0^{Y_{90}} (1 - C) \times dy} \tag{10a}$$

Flat impervious stepped weir

$$U_w = \frac{\int_0^{Y_{90}} (1 - C) \times V \times dy}{\int_0^{Y_{90}} (1 - C) \times dy} \tag{10b}$$

Gabion stepped weir

where q is the discharge per unit width at the weir crest. The coefficient of mass transfer K_L was shown to be constant regardless of bubble size and flow turbulence [21]:

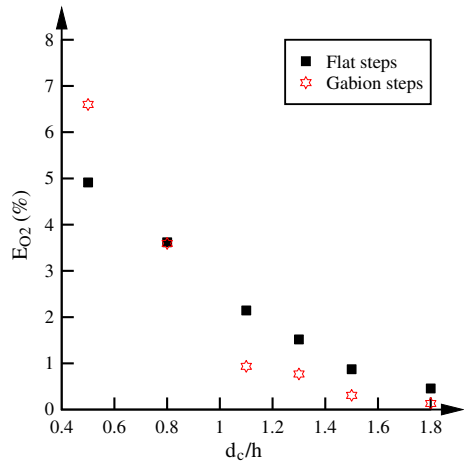
$$K_L = 0.47 \times \sqrt{D_{\text{gas}}} \times \sqrt[3]{g} \times \left(\frac{\mu_w}{\rho_w}\right)^{-1/6} \tag{11}$$

with μ_w the dynamic viscosity of water, ρ_w the density of water, g the gravity acceleration and D_{gas} the molecular diffusivity. Equation (11) was developed for bubble sizes larger than 0.25 mm in bubble column reactors. Its application to the highly turbulent stepped weir flows was justified since all detected bubbles were larger than 0.25 mm. For oxygen, the molecular diffusivity may be approximated by [15]:

$$D_{\text{gas}} (\text{O}_2) = 1.16793 \times 10^{-27} \times T_K^{7.3892} \tag{12}$$

where T_K is the temperature in Kelvin. For $T_K = 293\text{K}$, the mass transfer coefficient K_L equals: $K_L = 4.37 \times 10^{-4}\text{m/s}$. Herein the re-oxygenation transfer rate was derived from the integration of the mass transfer equation (9) based upon the air–water properties. The

Fig. 9 Aeration efficiency of the gabion and flat impervious stepped weirs ($\theta = 26.6^\circ$, $h = 0.10\text{m}$)—calculations performed at step edge 10 in terms of re-oxygenation rate



calculations were performed for both gabion and flat impervious stepped weirs for a range of discharges in terms of dissolved oxygen at 20 Celsius, standard pressure and zero salinity. The results are presented in terms of the aeration efficiency E of the stepped weir defined as:

$$E = \frac{C_{DS} - C_{US}}{C_{SAT} - C_{US}} \tag{13}$$

where C_{US} and C_{DS} are respectively the upstream and downstream dissolved oxygen concentrations. The results showed that the gabion stepped chute had a greater aeration efficiency for the lowest discharges ($d_c/h = 0.5$) (Fig. 9). Little difference between gabion and flat and gabion stepped weir were seen in the transition flow ($d_c/h = 0.8$). In skimming flow regime ($d_c/h > 0.9$), the re-oxygenation rate was substantially larger on the flat impervious stepped chute (Fig. 9). Figure 10 shows the aeration efficiency per metre drop in invert elevation as a function of the measured rate of energy dissipation $\Delta H/H_{max}$, where ΔH is the head loss down the stepped chute and H_{max} is the upstream total head. The data are compared with a number of air–water flow studies and with some dissolved oxygen measurements on flat stepped weirs. The details of studies are listed in the figure caption. Overall, the gabion stepped weir results compared well with the simple correlation proposed by [13]:

$$\frac{E}{\Delta z_0} = 0.15 \times \left(\frac{\Delta H}{H_{max}} \right)^{2.6} \tag{14}$$

where E is the total aeration efficiency in terms of dissolved oxygen and Δz_0 is the drop in elevation. Equation (14) is compared with experimental results in Fig. 10. The results implied a monotonic increase in re-oxygenation rate with increasing rate of energy dissipation on a stepped weir.

5.3 Discussion

A comparison with previous data showed a good agreement for stepped channels with slopes within $3.4^\circ < \theta < 26.6^\circ$, highlighting a monotonic increase in re-aeration with increasing rate of energy dissipation (Fig. 10). Large specific interface areas were recorded with depth-averaged values up to 200m^{-1} , although lesser specific interface areas were measured on the gabion stepped chute.

Reference	θ (°)	h (m)	Data	Instrumentation	Comments
CHANSON & TOOMBES (2002)	21.8	0.10	Calculations	Single-tip probe (\varnothing -0.35 mm)	Flat impervious steps
			Calculations	Dual-tip probe (\varnothing -0.025 mm)	Flat impervious steps
TOOMBES & CHANSON (2005)	3.4	0.143	DO measurements	TPS90 FLMV	Flat impervious steps
			Calculations	Dual-tip probe (\varnothing -0.025 mm)	Flat impervious steps
FELDER & CHANSON (2009)	21.8	0.10	Calculations	Dual-tip probe (\varnothing -0.25 mm)	Flat impervious steps
BUNG & SCHLENKOFF (2010)	26.6	0.06	DO measurements	WTW Oxi320	Flat impervious steps
Present study	26.6	0.10	Calculations	Dual-tip probe (\varnothing -0.25 mm)	Flat impervious steps
					Gabion steps

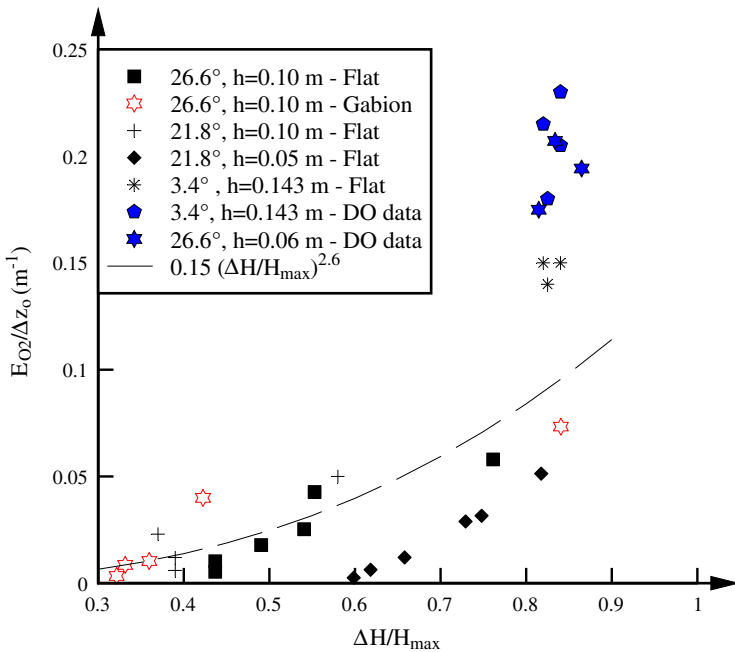


Fig. 10 Aeration efficiency per metre drop in invert elevation $E/\Delta z_0$ in terms of dissolved oxygen at 20 °C—comparison between air–water flow data obtained from the integration of the mass transfer equation and dissolved oxygen measurements

The integration of Fick’s law based upon detailed air–water flow measurements allowed a comparison between gabion and flat impervious stepped weirs in terms of aeration performances. The results showed that, for a small discharge, the aeration efficiency was higher on the gabion stepped chute, whereas, for large discharges, the flat impervious stepped weir was more efficient in terms of aeration and mass transfer. The present results were consistent with the data of [3] (Fig. 10).

It must be acknowledged that the above calculations were performed in the overflow and neglected the mass transfer rate in the gabion seepage flow. Since the present observations highlighted a substantial bubbly flow motion in the gabions, the above re-aeration calculations for gabion stepped weirs might underestimate the overall re-oxygenation potential of gabion stepped spillways.

6 Conclusion

The aeration performances of gabion stepped weirs were investigated physically through a comprehensive physical study based upon a Froude similitude. Three gabion stepped weirs and a flat impervious stepped weir were tested in a relatively large size facility with a 26.6° chute slope. The gabion stepped chutes consisted of ten gabion boxes filled with 14 mm sieved gravels, stacked above the flat impervious stepped chute. For two configurations, some horizontal step cappings were added. For all configurations, detailed air–water flow measurements were performed on the chute centreline for a range of discharges corresponding to Reynolds numbers between 3.8×10^4 and 8.7×10^5 .

In the gabion structures and for all flow conditions, the observations highlighted the interactions between seepage and overflow, including a bubbly motion in the gabion boxes. The air–water flow measurements showed comparable trends for all stepped weirs, although with some quantitative differences. Overall the gabion stepped chute was less aerated, the air–water specific area was slightly lower on the gabions stepped weir, and larger velocities were measured at the downstream end of the gabion stepped chute. The air–water properties of the capped and fully-capped gabion stepped weirs were typically intermediate between the flat impervious and gabion stepped chute flow properties.

The aeration efficiency of gabion and flat stepped weirs was derived from the integration of Fick's law based upon the specific interfacial area measurements. For the lowest discharge, the aeration performances of the gabion stepped configuration were enhanced. In skimming flows, the aeration efficiency of the flat impervious stepped weir was larger than that of the gabion stepped chute.

In conclusion the present study focused on gabion stepped weirs with and without capping. Using physical modelling performed under controlled flow conditions, the observations showed the significant interactions between the seepage and overflow. For large discharges, lower performances were observed in terms of energy dissipation and aeration efficiency on the gabion stepped weir, in comparison to the performances of flat impervious stepped weir. This counter-intuitive result on the gabion stepped weir emphasised the importance of sound physical modelling in the investigations of hydraulic structures.

Acknowledgments The authors acknowledge the technical of Jason VAN DER GEVEL and Matthews STEWART, School of Civil Engineering at the University of Queensland. The financial support of the Australian Research Council (Grant DP120100481) is acknowledged.

Appendix 1: Relationship between void fraction and bubble count rate in self-aerated flows

In self-aerated chute flows, the relationship between void fraction and bubble count rate tends to follow a pseudo-parabolic relationship close to [4,8,31]:

$$\frac{F}{F_{\max}} = 4 \times C \times (1 - C) \quad (15)$$

where F_{\max} is the maximum bubble rate in a cross-section. A more advanced theoretical model was introduced by [31] and [33]:

$$\frac{F}{F_{\max}} = \frac{1}{\alpha \times \beta} \times \frac{C \times (1 - C)}{C_{F_{\max}}^2} \tag{16}$$

where α and β are two correction factors which are functions of the local void fraction and flow conditions, and $C_{F_{\max}}$ is the void fraction for which $F = F_{\max}$. The first correction parameter α accounts for the different average sizes of air bubble chord size λ_a and water droplet chord size λ_w :

$$\alpha = 1 + \left(\frac{\lambda_w}{\lambda_a} - 1 \right) \times C \tag{17}$$

with the ratio λ_w/λ_a assumed to be constant within a cross-section and independent of the void fraction. The second correction factor β takes into account the variation of λ_w and λ_a with the void fraction:

$$\beta(C) = 1 - b \times (1 - 2 \times C)^4 \tag{18}$$

where b is a characteristic value of the maximum variation of β : i.e., $1 - b < \beta < 1$ [33]. Some typical results are presented in Fig. 7 where Eqs. (15) and (16) are compared with experimental data. Equation (16) compared favourable with the data on both flat impervious and gabion stepped configurations. The best agreement was found for $\lambda_w/\lambda_a = 2.4$ and $b = 0.55$ for the flat impervious stepped configuration. and for $\lambda_w/\lambda_a = 1.6$ and $b = 0.52$ for the gabion stepped configuration. The values were generally in agreement with the findings of [12] for the same chute slope.

References

1. Agostini R, Bizzarri A, Masetti M, Papetti A (1987) Flexible Gabion and Reno Mattress structures in river and stream training works, 2nd edn. Section one: Weirs. Officine Maccaferri, Bologna, Italy.
2. Boes R, Schmid H (2003) Weir rehabilitation using gabions as a noise abatement option. In: Proceedings of the HYDRO-2003 conference, Cavtat, pp 781–785
3. Bung DB, Schlenkhoff A (2010) Self-aerated flow on embankment stepped spillways: the effect of additional micro-roughness on energy dissipation and oxygen transfer. In: Proceedings of the 1st IAHR European Congress, p. 6. 4–6 May, Edinburgh (CD-ROM)
4. Chanson H (1997) Air bubble entrainment in open channels. Flow structure and bubble size distributions. *Int J Multiph Flow* 23(1):193–203
5. Chanson H (2001) The hydraulics of stepped chutes and spillways. Balkema, Lisse, p 384
6. Chanson H (2002) Air–water flow measurements with intrusive phase-detection probes. Can we improve their interpretation? *J Hydraul Eng ASCE* 128(3):252–255
7. Chanson H (2009) Turbulent air–water flows in hydraulic structures: dynamic similarity and scale effects. *Environ Fluid Mech* 9(2):125–142. doi:10.1007/s10652-008-9078-3
8. Chanson H, Toombes L (2002) Experimental study of gas–liquid interfacial properties in a stepped cascade flow. *Environ Fluid Mech* 2(3):241–263
9. Chanson H, Toombes L (2004) Hydraulics of stepped chutes: the transition flow. *J Hydraul Res* 42(1):43–54
10. Chanson H, Yasuda Y, Ohtsu I (2002) Flow resistance in skimming flows and its modelling. *Can J Civ Eng* 29(6):809–819
11. Corsi R, Madani-Isfahani M, Zytner R (1992) Oxygen transfer and VOC emissions from sewer drop structures. *Water Environ Res* 69(3):286–294
12. Felder S (2013) Air–water flow properties on stepped spillways for embankment dams: aeration, energy dissipation and turbulence on uniform, non-uniform and pooled stepped chutes. Ph.D. thesis, The University of Queensland, School of Civil Engineering, Brisbane, p. 506

13. Felder S, Chanson H (2009) Energy dissipation, flow resistance and gas–liquid interfacial area in skimming flows on moderate-slope stepped spillways. *Environ Fluid Mech* 9(4):427–441
14. Felder S, Chanson H (2012) Free-surface profiles, velocity and pressure distributions on a broad-crested weir: a physical study. *J Irrig Drain Eng* 138(12):1068–1074
15. Ferrell RT, Himmelblau DM (1967) Diffusion coefficients of nitrogen and oxygen in water. *J Chem Eng Data* 12(1):111–115
16. Gasparotto R (1992) Waterfall aeration works. *Civ Eng ASCE* 62(10):52–54
17. Gonzalez C, Takahashi M, Chanson H (2008) An experimental study of effects of step roughness in skimming flows on stepped chutes. *J Hydraul Res* 46(1):24–35
18. Gosse P, Gregoire A (1997) Dispositif de Réoxygénation Artificielle du Sinnamary à l’Aval du Barrage de Petit-Saut (Guyane)*. (*Artificial Re-Oxygenation of the Sinnamary, Downstream of Petit-Saut Dam (French Guyana)*.) *Hydroécol Appl Tome 9*. 1–2:23–56 (in French)
19. Hauser GE, Shane RM, Niznik JA, Brock WG (1992) Innovative reregulation Weirs. *Civ Eng ASCE* 62(5):64–66
20. Gulliver JS (1990) Introduction to air–water mass transfer. In: Wilhelms SC, Gulliver JS Proceedings of the 2nd international symposium on gas transfer at water surfaces, air–water mass transfer, ASCE Publ., Minneapolis, pp 1–7
21. Kawase Y, Moo-Young M (1992) Correlations for liquid-phase mass transfer coefficients in bubble column reactors with Newtonian and non-Newtonian fluids. *Can J Chem Eng* 70:48–54
22. Kells JA (1993) Spatially varied flow over rockfill embankments. *Can J Civ Eng* 20:820–827
23. Knauss J (1995) ΤΗΣ ΓΡΙΑΣ ΤΟ ΠΗΔΗΜΑ, der Altweibersprung. Die Rätselhafte Alte Talsperre in der Gloses-Schlucht bei Alyzeia in Akarnanien. *Archäologischer Anzeiger* 5:138–162
24. Matos J (2001) Onset of skimming flow on stepped spillways. Discussion. *J Hydraul Eng ASCE* 127(6):519–521
25. Nakasone H (1987) Study of aeration at Weirs and cascades. *J Environ Eng ASCE* 113(1):64–81
26. Novak P, Moffat AIB, Nalluri C, Narayanan R (2001) *Hydraulic structures*, 3rd edn. Spon Press, London, p 666
27. Peyras L, Royet P, Degoutte G (1991) Ecoulement et Dissipation sur les Déversoirs en Gradins de Gabions. (*Flows and Dissipation of Energy on Gabion Weirs*) *J La Houille Blanche* 1:37–47 (in French)
28. Pfister M, Chanson H (2012) Scale effects in physical hydraulic engineering models. Discussion. *J Hydraul Res IAHR* 50(2):244–246. doi:[10.1080/00221686.2012.654672](https://doi.org/10.1080/00221686.2012.654672)
29. Rajaratnam N (1990) Skimming flow in stepped spillways. *J Hydraul Eng ASCE* 116(4):587–591
30. Stephenson D (1979) Gabion energy dissipators. In: Proceedings of the 13th ICOLD congress, New Delhi, Q. 50. R 3:33–43
31. Toombes L (2002) Experimental Study of air–water flow properties on low-gradient stepped cascades. Ph.D. Thesis, University of Queensland, School of Civil Engineering, Brisbane, pp 304
32. Toombes L, Chanson H (2005) Air–water mass transfer on a stepped spillway. *J Environ Eng* 131(10):1377–1386
33. Toombes L, Chanson H (2007) Surface waves and roughness in self-aerated supercritical flow. *Environ Fluid Mech* 7(3):259–270. doi:[10.1007/s10652-007-9022-y](https://doi.org/10.1007/s10652-007-9022-y)
34. Wood IR (1991) Air entrainment in free-surface flows. IAHR hydraulic structures design Manual No. 4, Hydraulic Design Considerations, Balkema Publications, Rotterdam, pp 149
35. Wuthrich D, Chanson H (2014) Aeration and energy dissipation over stepped Gabion spillways: a physical study. Hydraulic Model Report No. CH92/13, School of Civil Engineering, The University of Queensland, Brisbane, pp 171 and 5 video movies (ISBN 9781742720944)